National Technical University of Athens

Interdisciplinary Postgraduate Programme

Design & Construction of Underground Works

Investigating the interaction of land subsidence and flooding phenomena in coastal areas of Greece with the use of Interferometry Techniques and ground truth data. The cases of Messolonghi and Aitolikon.

Master's thesis

Antoniadis Nikolaos

Supervisor: Constantinos Loupasakis,

Professor, N.T.U.A.

Athens, 2023

ABSTRACT

Land subsidence is a major threat in urban areas. Continuous vertical displacements over time can severely damage linear infrastructures, such as bridges, road networks, railways, and pipelines, and create serious building stability problems when differential settlements occur. This ground deformation phenomenon may occur as a consequence of natural processes, such as organic soils oxidation [1,2], the collapse of underground cavities [3-5], and natural compaction [6], or due to anthropogenic processes, such as groundwater overexploitation [7-12] or as a combination of both natural and anthropogenic processes. Another phenomenon manifested in coastal areas and presented in this study is flooding. Sea level rise (SLR) accompanying climate change has begun to cause significant damage in coastal areas around the world.

The detection, measurement, and monitoring of land subsidence are crucial for both urban areas and infrastructures. Interferometric Synthetic Aperture Radar (InSAR) is a well-established method for monitoring ground displacement phenomena and is successfully applied in a variety of Earth deformation studies around the world and Greece. Numerous land subsidence sites in Greece have been detected and analyzed using InSAR techniques [13-32].

The current study focused on land subsidence phenomena along the coastal areas of Messolonghi and Aitolikon during the last decade, using the Persistent Scatterer (PSI) interferometry technique and ground truth data. The Persistent Scatterers interferometry technique was implemented in Sentinel-1 SLC images from 2015 to 2021 to perform a time series analysis of the line-of-sight (LOS) displacements in the affected areas. The parallelized PSI (P-PSI) processing chain [33], developed in the Operational Unit BEYOND Center for EO Research and Satellite Remote Sensing of the National Observatory of Athens (NOA), was used for the processing of SAR data and the extraction of the LOS deformation field. The estimated LOS displacements verified the land subsidence phenomena in both sites. The velocities of permanent scatterers, combined with the geological, geotechnical, and hydrogeological data, validated the observed Permanent Scatterers' negative velocities and enabled a more accurate interpretation of the phenomenon

The city of Messolonghi is surrounded by the homonymous sea lagoon. The surrounding area consists primarily of cultivated land, while some swamps and saline soils can be seen around the lagoon and along the river deltas. Sandy islets on the front of the lagoons are a particularly sensitive morphological element crucial for preserving the lagoon system. On the other hand, Aitolikon is situated in the center of the Aitolikon Lagoon, 10 kilometers northeast of Messolonghi. Two 19th-century stone arched bridges, each approximately 300 meters long, connect it to the shore on both

the east and west sides. Aitolikon initially consisted of 4–5 very small islands in the center of a lagoon, which were completely submerged during the winter. The first attempts to link the islands were conducted by fishermen using wooden piles and earth fills. Over the years, continuous filling was added, resulting in the formation of an irregularly shaped island 300 m in diameter. The last filling was added in 1969, with particular attention paid to the north and south sides. The addition of fillings enabled the building of more houses in the reclaimed area. However, the north side especially presented major problems as the buildings' foundations were under the water.

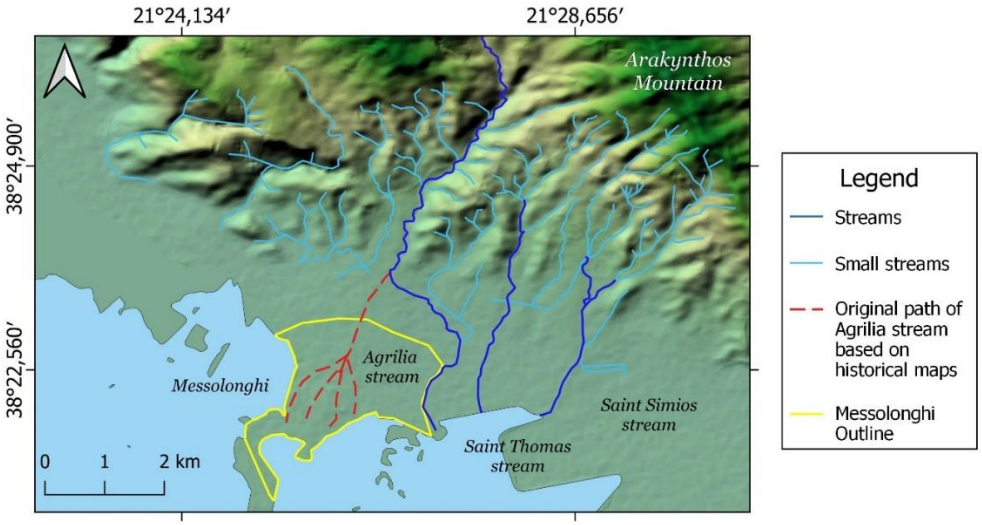

Figure 1. Hydrographical map of Messolonghi greater area

Regarding the geological setting of Messolonghi, the city occupies a flat lowland and is founded on Quaternary alluvial deposits consisting of fine grain sediments (clays, silts, and sands). The stream of Agrilia, originating from the Arakynthos mountain, has been the main provider of fluvial deposits of the Messolonghi narrow site. Currently, the stream travels along its natural course until it is forced to loop around the city (Figure 1). It is believed that the area's first settlers changed the course of the river, preventing the city from flooding. In this case, diverting the stream has prevented the river sediments from reaching the coastal areas, and thus the natural land subsidence has not been offset by the sediment accumulation.

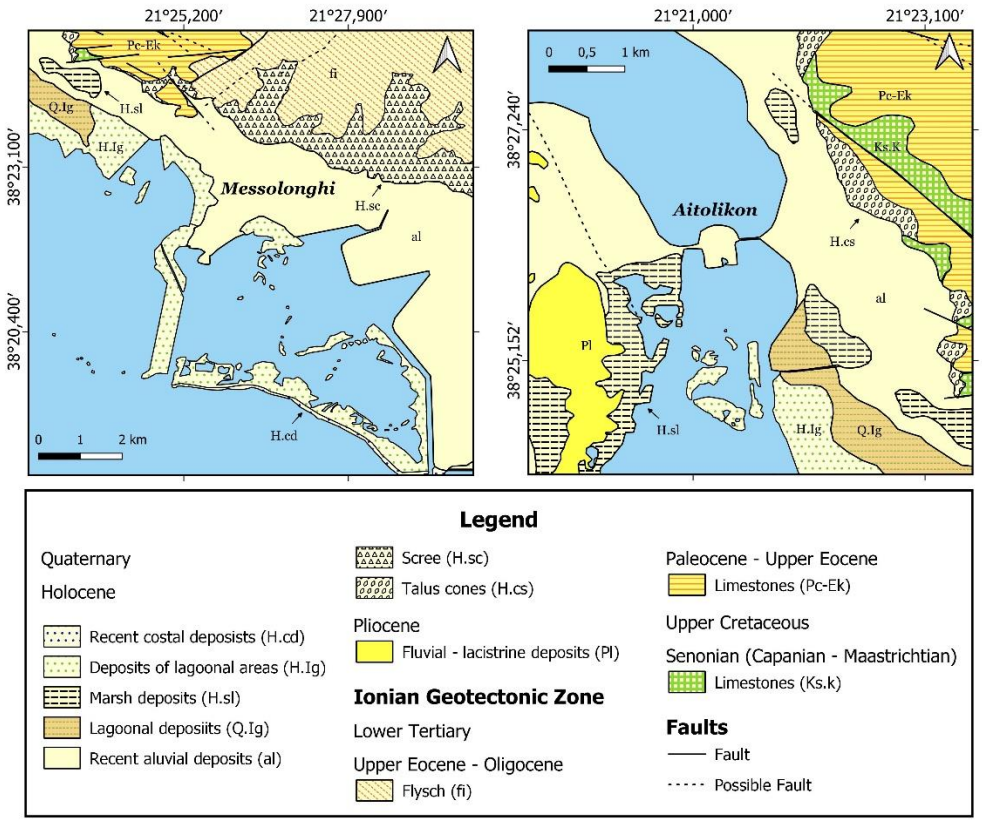

Figure 2. Geological maps of the Messolonghi (left) and Aitolikon (right) modified by Hellenic Survey of Geology & Mineral Exploration (HSGME) (1987–1990)

According to data obtained from geotechnical boreholes, the Quaternary formations consist of recent alluvial deposits (Figure 2). The loose Quaternary coastal deposits extend horizontally along the site consisting of soft clay horizons intercalated with sandy silt to silty sand and silt, reaching down to a maximum depth of approximately 100 m. Focusing on the top layers bearing loads of the buildings, there are several fine-grain layers in continuous alternation, including an organic clay layer with a varying thickness of 5–10 m, organic clayey silt to silt layer, 5–10 m thick, and a clayey sand to sand layer with a thickness of 2–3 m (Figure 3b). The organic clay layer contains a significant amount of plant residue and limestone fragments. Investigations of the soil formations in the greater Messolonghi area revealed that the clay layers are rich in shell and biogenic particles [34]. The content of organic material in the clay layers is significant, ranging from 5 to 13%. In several locations in the city, the organic clay horizon is located above the water level, thus manifesting in the oxidation of the layer's organic content. According to the geological maps by the Hellenic Survey of Geology and Mineral Exploration (HSGME), the Pliocene deposits have a thickness of 80–100 m. Underlying that formation is the flysch with a thickness of 1200–1400 m, followed by the Paleocene and Senonian limestone with a thickness of 300–400 m.

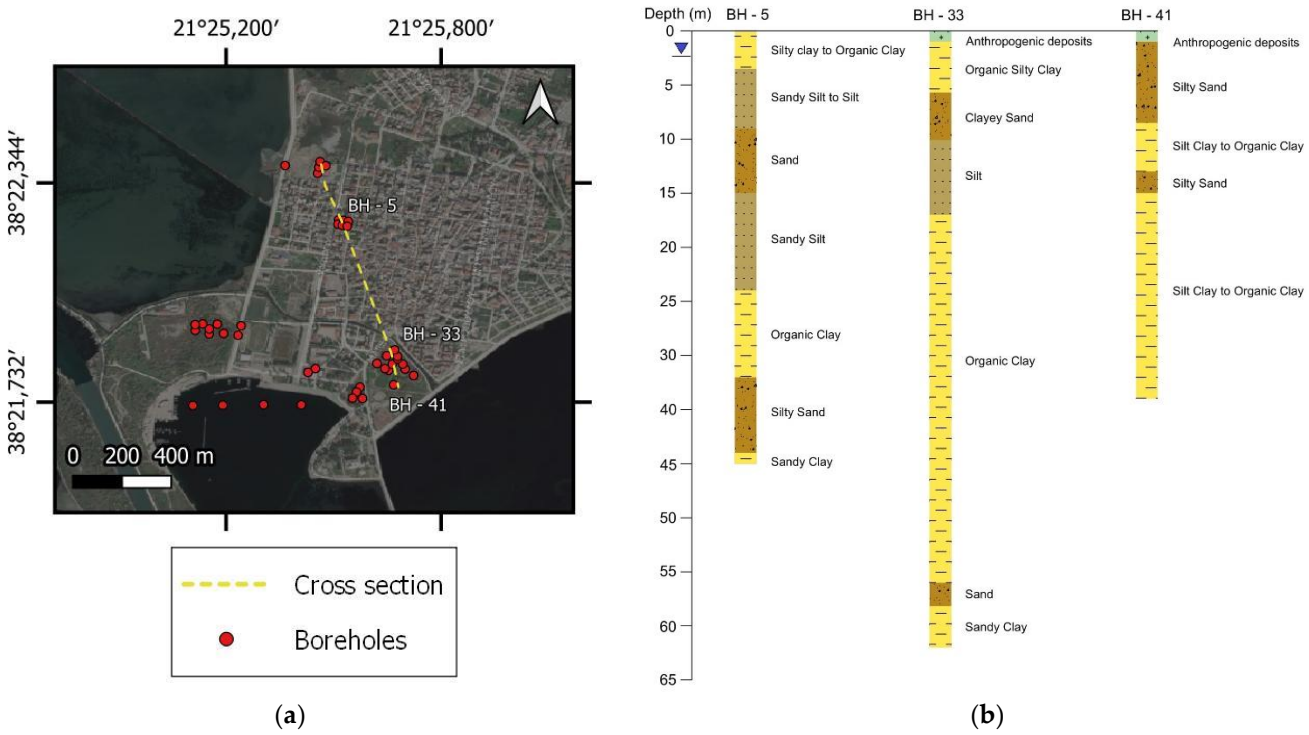

Figure 3. (a) Geotechnical borehole locations in Messolonghi (b) Indicative logs along the cross section of (a).

A total of 44 drilling profiles (Figure 3a) and over 100 oedometer tests were collected for the city of Messolonghi from the Hellenic Survey of Geology and Mineral Exploration [35,36], the Central Laboratory of Public Works archives [37,38], and private geotechnical consultants` reports [39]. These data were analyzed and statistically processed. According to the test results, all layers detected in the study area are highly compressible, presenting high to very high compression index (C_c) values ranging from 0.187 to 0.467. Additionally, as indicated by the low standard penetration test values (N_{SPT}), they can be described as very soft to moderately stiff. For instance, the organic clay layers of the coastal deposits, constituting most of the formations, can be identified with SPT values between 3 and 18.

In the broader Messolonghi area, there are two aquifer systems, a karstic aquifer system within the Alpine–pre-Alpine bedrock formations (Pc-Ek and Ks.k) and the one developed in the Quaternary formations, occupying the wider plane area extending west of Messolonghi. The shallow unconfined aquifer recharges by both lateral karstic water overflow along the foothill and through the scree and by filtration of surface water, which fluctuates due to the mean sea level rise. Nonetheless, previous boreholes indicated the mean groundwater level inside the city of Messolonghi at around 2 m below the surface. According to the groundwater contour lines, the aquifer flows from the foothills of the Arakynthos mountain, behind the study area, and to the south–southwest toward the coastline. This aquifer also recharges the permeable phase of the flysch. A previous hydrochemical study has

identified increased salinity in the groundwater toward the coastline, which can be related to seawater intrusion and possibly the dissolution of the salt content of the sediments [34]. In Aitolikon, the hydrogeological conditions are predictable. The lagoon water penetrates the earth fill material, and the groundwater level can be identified as 1.0 to 1.5 m under the ground, at the sea surface level.

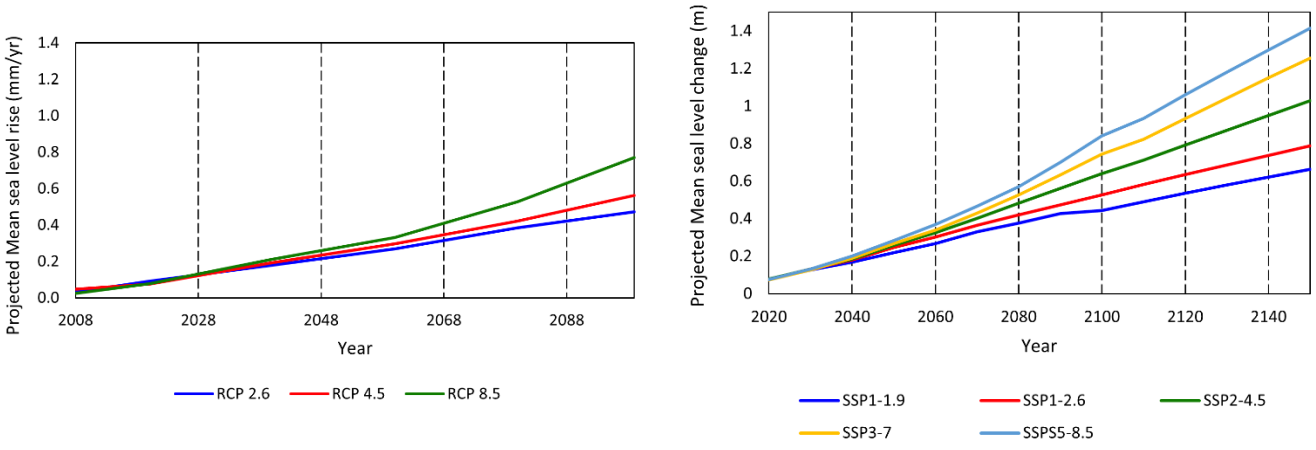

(**a**) (**b**)

Figure 4. (a) Projected Mean Sea level change in coastal Greece according to RCP scenarios (b). Projected Mean Sea level change at Messolonghi lagoon according to the SSP scenarios

The recent escalation of global warming and climate change has led to an increase in abnormal global weather patterns and extreme hydrological phenomena. In the case of Messolonghi and Aitolikon, these phenomena have frequently resulted in natural disasters such as floods. Thus, climate change has increased the frequency and volume of precipitation in the study area and caused a sea level rise. Katakolon tidal gauge, located 81 km from the study area, recorded a 2.09 mm/year sea level rise from 1970 to 2021, adding up to a total increase of 11 cm since the 1970s. However, the tidal gauge in Patras' port, 32 km from the study area, recorded a higher sea level rise in the gulf of 7 mm/year from 2017 to 2021 [40,41]. These finding make it clear that the sea level is rising. The continuous sea level rise can be interpreted as one of the main causes for the reported rush of seawater over the lowlands. The Representative Concentration Pathway (RCP) and Shared Socioeconomic Pathways (SSP) scenarios can be used to estimate the projected sea level rise. RCPs describe different levels of greenhouse gases and other radiative forcings that might occur in the future. Four pathways were developed, covering a broad spectrum of forcing in 2100 (RCP 2.6, RCP 4.5, RCP 6.0, and RCP 8.5 watts per meter squared). However, the RCP scenarios did not include socioeconomic factors and their change over the next century. These factors were examined in the SSPs and included variables such as population, economic growth, education, urbanization, and the rate of technological development. They evaluated five different ways in which the world might evolve in the absence of climate policy

and how various levels of climate change alleviation can be achieved when the mitigation goals of RCPs and SSPs are combined. The projected mean sea level rise for coastal Greece and the Messolonghi lagoon based on these scenarios were found. The RCP2.6 model, the lowest baseline emissions scenario, indicates a 0.5 m mean sea level rise of coastal Greece over the next 80 years, while RCP 8.5, the highest baseline emissions scenario, indicates 0.77 m (Figure 4) [42]. If a very high-emissions scenario (SSP5-8.5) is considered, then the mean sea level in the Messolonghi lagoon is expected to rise to 0.85 m by 2100. The constant increase in the sea level has been causing a rush of seawater over the Messolonghi and Aitolikon lowlands. The situation is expected to worsen over the next few years because of the gradual subsidence of the sites and the increase in the mean precipitation rates caused by climate change, resulting to sections of Messolonghi and Aitolikon being flooded by 2100 [43].

The precipitation data obtained from the automatic weather stations' NOANN network of the National Observatory of Athens (NOA) [44] for the Aitolikon weather station were statistically processed and analyzed to obtain the mean monthly and yearly precipitation rates. For the examined period (2015–2022), monthly rainfall values varied from 0 to 357 mm, while the average annual precipitation was 750 mm/yr. The most significant rainfalls were mainly concentrated between October and February, where the average precipitation rate was 133 mm. As mentioned, rainfalls were significantly high during the wet period, leading to difficulties in draining river flow discharge and increased water levels. The maximum inundated area has increased each year because of the intensification of the precipitation volume and the rising sea level, causing several floods.

As it was prementioned, for the present study, the Stanford Method for Persistent Scatterers (StaMPS) [45] was implemented on Sentinel-1 satellite data provided by the Hellenic Mirror Site and the Sentinel Greek Copernicus Data Hubs [46], enabling small-scale surface deformation monitoring over an extended period. Additionally, to reduce the atmospheric impact on the estimated LOS displacements, a phase-based linear correction was implemented on the produced Sentinel-1 interferograms using the open-source Toolbox for Reducing Atmospheric InSAR Noise (TRAIN) [47]. A total of 161 and 120 Sentinel-1A and 1B SLC images from the Copernicus program, of both descending and ascending satellite passes, were processed with the parallelized Persistent Scatterer Interferometry (P-PSI) processing chain, developed in the unit BEYOND Center of EO Research and Satellite RS of the IAASARS/NOA. The estimated line-of-sight (LOS) displacements provided insights into the considerable continuing hazard in the areas of interest. Vertical displacements were estimated for both the ascending and descending track and were compared to the results presented by the Copernicus European Ground Motion Service. The standard deviation values for the descending and ascending track were 0.4-0.62 mm/year for the descending and

0.33-0.58 mm/year for the ascending track, respectively. Furthermore, the information provided by the European Ground Motion Service (EGMS) was evaluated. The EGMS is the largest wide-area A-DInSAR service ever conceived [48,49]. This initiative was defined in the period 2016–2017 and finalized in 2017. The same year, it was approved by the Copernicus user forum and the Copernicus committee. The EGMS aims to provide reliable information regarding natural and anthropogenic ground motion phenomena over Europe for the study of geohazards and human-induced deformation such as slow-moving landslides, subsidence due to groundwater exploitation or underground mining, volcanic unrests and many more. This goal is achieved through the use of Sentinel-1A and 1B SAR images, received from two different look angles (ascending and descending), with a revisit time of six days, processed at full resolution. In order to evaluate and validate the spatial distribution of the subsidence, it was necessary to correlate it with ground truth data. The geological and geotechnical data acquired from maps, technical reports, and drilling profiles enabled the validation and interpretation of the PSI results, and thus, a more holistic and temporally complete view of the phenomenon was achieved.

Figure 5. Damages recorded in buildings due to deferential deformations. South side balcony damage in Building D

Extensive field campaigns were carried out in both cities, where damage to several buildings was recorded. Numerous buildings were affected by the subsiding phenomena, including the Prefectural Administration of Aitoloakarnania, the Port Authority, the Public Finance Service of Messolonghi, and many residential buildings. Significant damages were also found in the older buildings, throughout Messolonghi (Figure 5).

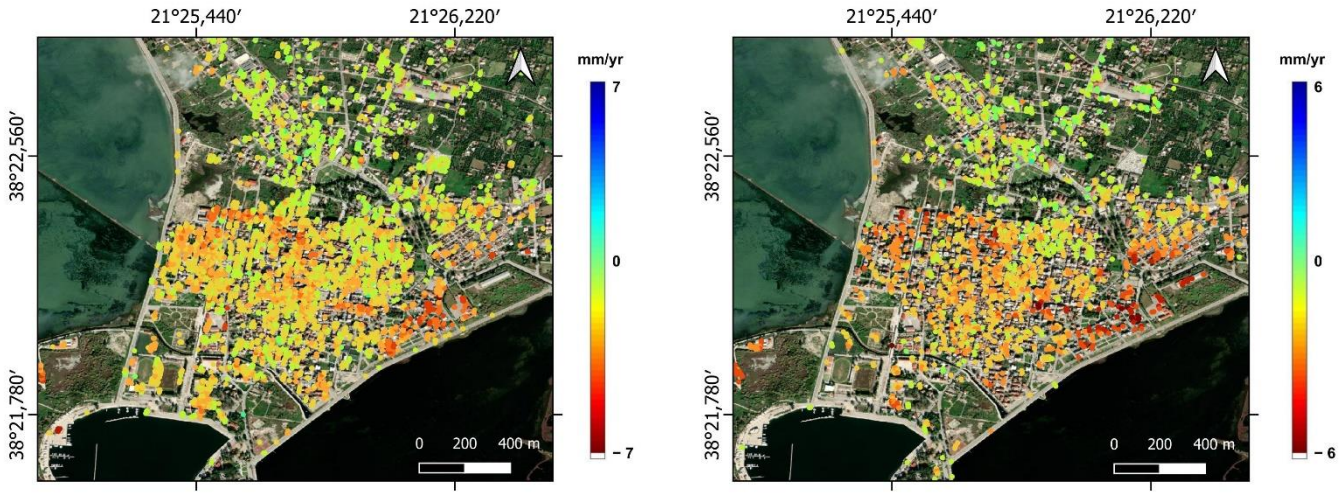

Figure 6. Spatial distribution of the Sentinel-1 vertical deformations in Messolonghi for (a) the descending satellite pass (no. 80) & (b) the ascending satellite pass (no. 175). Both coming from the P-PSI satellite data analysis conducted at BEYOND.

To successfully interpret the dominant mechanisms behind the subsidence phenomena recorded in both cities, all factors that may have affected their evolution were evaluated (geological, geotechnical, and hydrogeological data, remote sensing data, sea rise data, and precipitation rates).

The town of Messolonghi presents a variety of vertical deformation rates. Maximum displacement values in the vicinity of Messolonghi are of the order of −5 mm/yr (Figure 6). The Persistent Scatterers (PSs) indicated relatively stable ground conditions in the northern part of the town during the investigated time period as the vertical values ranged from 0.3 to 1.3 mm/year. However, the recorded deformations were increased in other parts of the town. Subsiding Persistent Scatterers were concentrated along the coastal zone, with a higher density east of the town (mean deformation rate of −5 mm/yr). The south and west parts of the town also presented a mean subsidence rate of −2.5 mm/yr and −3 mm/yr, respectively. The mean vertical deformation rates provided by the Copernicus European Ground Motion Service were around −4.5 mm/yr. The NOA analysis and the EGMS data were in perfect agreement as, in both datasets, the spatial distribution of the deformations was the same and the northern part of the town presented the highest deformation rates.

As indicated, the city is built on compressible soil, probably under consolidated formations subjected to subsidence caused by the external construction loads, leading to foundation settlement. Most buildings in Messolonghi are built with mat foundations and only a few with spread footings. Deformation patterns are manifested primarily in buildings constructed with the former type of foundation. Moreover, as mentioned, in several locations in the city, the organic clay layer is situated above the water level, resulting in subsidence and the oxidation of the layer's

organic content. Secondary consolidation might also be considered a factor leading to land subsidence in some parts of the study area, specifically the central part of Messolonghi. Even though the buildings in that area were constructed during the 1950s, vertical displacements still manifest today. It can be assumed that the primary consolidation was exhausted, and the secondary consolidation (creep) is now manifesting. However, another explanation is that, due to the constant increase in the sea level and the increased precipitation rates, the groundwater level fluctuates throughout the year, leading to the reactivation of the primary consolidation.

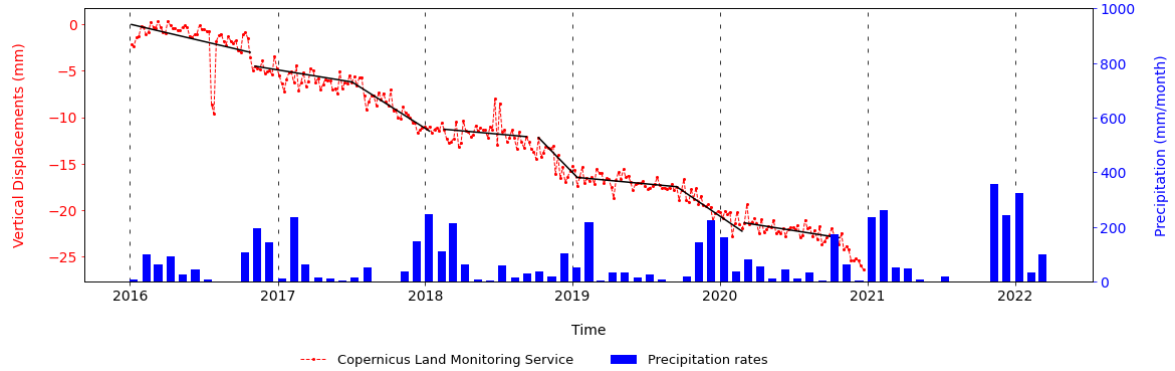

Figure 7. Displacements recorded vs precipitation rates for the Prefectural Administration of Aitoloakarnania building (B). Each blue bar represents the precipitation rates for 1 month. Vertical displacements in the form of time-series from the European Ground Motion Service of Copernicus. Trend lines (black color) indicate the changes on the subsidence rate.

The time series of the deformations referring to the PSs located on almost all the damaged buildings follow a specific pattern (Figure 7). At the beginning of the wet season (October–November), the deformations appear to slow down, and they start accelerating in the middle of the dry season (June). It seems that the recharge of the aquifers during the wet period (from September to June) increased the groundwater pore pressure and, with a short time offset from the beginning of the rainfalls, led to the deceleration of the subsidence. Conversely, the draining of the aquifers during the dry period (May-September) reduced the groundwater pore pressure leading to the acceleration of the deformations, also with a short time offset from the beginning of the draining. The time offset, in either case, was not fixed, depending on the intensity of the rainfalls or the severity of the pumping activities that occurred each year. The above discussion proves that the natural recharge of the aquifers caused a slight alteration in the deformation trends of the land subsidence, decelerating the deformations. Nevertheless, it is clear that the seasonal fluctuation of the groundwater head could not affect the overall continuous subsiding trend witnessed through the time series.

To determine whether the aquifer has been subjected to overexploitation during the past years, the groundwater level measurements conducted during the hydrological year (October 2005–April 2006) were compared with measurements conducted by the HSGME from 2015 to 2022. The monitoring boreholes included in the current HSGME

network [50] are insufficient for producing new groundwater level contour maps, referring to the recent measurements (2015–2022). Therefore, measurements from neighboring boreholes of the two networks were compared to arrive at a conclusion concerning the possibility of an extensive groundwater discharge. By comparing the measurements conducted at the neighboring boreholes it is clear that the groundwater level has remained practically stable since 2005. Following the above discussion, it can be concluded that there is no deformation, due to the overexploitation of the aquifers currently at this particular site.

According to Corine's land use map for 2006 [51] and 2018 [52], there has been an increase in the area used for residential and commercial purposes in Eastern Messolonghi. This change supports the findings of the P-PSI analysis, which indicated that the affected area's subsidence rate, is the highest in the greater area of Messolonghi, as already mentioned. Due to the recent construction of the buildings in that area, it was possible to record the deformations imposed, by their loads. An increase of the areas used for industrial and commercial purposes is also visible in the eastern section of Messolonghi, which extends towards the national road. The PS points demonstrate how the deformation induced by the exploitation of the underground water and building loads, is now beginning to manifest.

Greece is a highly tectonic zone, and earthquakes have occurred throughout the examined time period. Nonetheless, the rock background and faults are located behind the study area and the earthquakes were only up to a magnitude of 4 A. The faults did not become active. Subsidence caused by the earthquakes would have been evident in the time series as a sharp step after the event. Thus, subsidence cannot be attributed to tectonic causes.

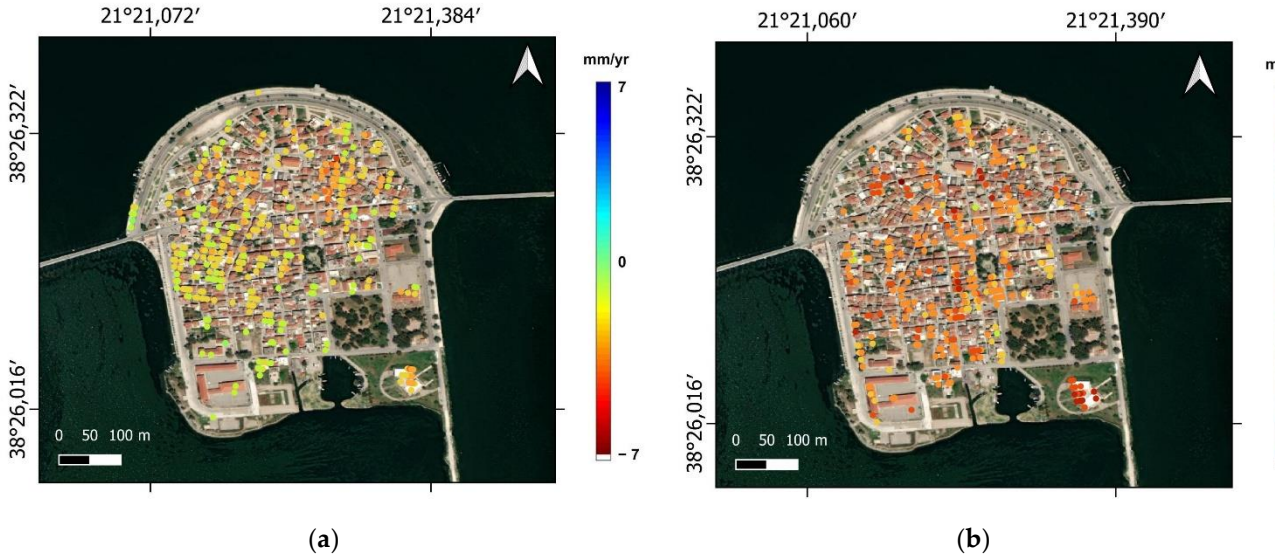

Figure 8. Spatial distribution of the Sentinel-1 vertical deformations in Aitolikon for (a) the descending satellite pass (no. 80) & (b) the ascending satellite pass (no. 175). Both coming from the P-PSI satellite data analysis conducted at BEYOND.

In Aitolikon, maximum vertical deformation values reach a mean rate of −4 mm/yr (Figure 8). Significant damages to old buildings have been recorded in the northern part of the town. It is worth mentioning that in that area, the houses' foundations were constructed in the water before the addition of the 1969 filling. The highest deformations were observed in the southern part of the island, where the Vaso Katraki Museum is located (mean values of −4.5 mm/year). The museum was constructed on top of the 1969 reclaimed area.

The time series of the deformations referring to the PSs located on almost all the damaged buildings indicate a continuous subsiding trend. At this particular site, sessional fluctuations related to the changes in the groundwater head, identical to those identified in Messolonghi, are not visible. The continuous subsiding trend can be viewed from the Copernicus European Ground Motion Service dataset and the P-PSI satellite data analysis conducted at BEYOND.

As no productive drills are exploiting the groundwater underneath Aitolikon, it is clear that the observed groundwater head fluctuation less than 1 m, due to the variations in the level of the lake, is not sufficient to affect the subsiding trend.

Unfortunately, geotechnical data referring to the geotechnical setting of Aitolikon are not available. Nevertheless, the fact that the entire city is founded over randomly deposited artificial fill leaves no doubt about the high compressibility of the formations leading to subsidence due to natural and external loads-induced compaction. It should also be mentioned that different motion rates were observed for nearby buildings, possibly caused by the different foundation types used and the heterogeneity of the filling materials. Following the above discussion, it is clear that the only cause of the land subsidence at Aitolikon is the natural compaction and the compaction due to the external loads exerted by the constructions.

Overall, it was found that the study areas, which were the coastal cities of Messolonghi and Aitolikon have been subjected to land subsiding phenomena. The present study provides an approach for identifying the subsidence mechanism by combining the geotechnical characteristics, hydrogeological data, sea level data, and precipitation data and verifying the displacements using space-borne SAR interferometry (InSAR) techniques and ground truth data. As observed, the subsiding deformation trend cannot be attributed to the exploitation of the groundwater level or tectonic causes. The coastal deposits occupying most of the study area were proven to be compressible due to the low compression index (C_c) values identified in all surface soil layers. Therefore, primary consolidation and natural compaction of the formations was the key factor leading to the land subsidence phenomena. On the other hand, sea level rise and precipitation rates, which have increased over the past few years due to climate change, are crucial factors that play a significant role in the repeated flooding of both

coastal cities. The manifestation of the deformations was verified using the space-borne SAR interferometry techniques conducted by the unit BEYOND Centre for Earth Observation Research and Satellite Remote Sensing of IAASARS/NOA and the Copernicus European Ground Motion Service. The results of the InSAR techniques were validated through field trips conducted in the affected areas, where building damage was documented. At the same time, the two coastal towns are affected by the constant sea level rise and a consequent rush of seawater. The situation is expected to worsen over the next few years, considering the combined effect of the gradual subsidence of the sites and the intensification of the meteorological phenomena caused by climate change.

References

1. Gambolati, G.; Putti, M.; Teatini, P. & Gasparetto Stori, G. Subsidence due to peat oxidation and impact on drainage infrastructures in a farmland catchment south of the Venice Lagoon. *Environmental Geology* **2006**, 49, 814–820, https://doi.org/10.1007/s00254-006-0176-6
2. Hoogland, T.; van den Akker, J. J. H., & Brus, D. J. Modeling the subsidence of peat soils in the Dutch coastal area. *Geoderma* **2012**, 171–172, 92–97, https://doi.org/10.1016/j.geoderma.2011.02.013
3. Caramanna, G.; Ciotoli, G. & Nisio, S. A review of natural sinkhole phenomena in Italian plain areas. *Natural Hazards* **2008**, 45, 145–172, https://doi.org/10.1007/s11069-007-9165-7
4. Galve, J. P.; Gutiérrez, F.; Lucha, P.; Guerrero, J.; Bonachea, J.; Remondo, J. & Cendrero, A. Probabilistic sinkhole modelling for hazard assessment. Earth Surface Processes and Landforms **2009**, 34, 437–452, https://doi.org/https://doi.org/10.1002/esp.1753
5. Ding, H.; Chen, S.; Chang, S.; Li, G. & Zhou, L. Prediction of Surface Subsidence Extension due to Underground Caving: A Case Study of Hemushan Iron Mine in China. *Mathematical Problems in Engineering* **2020**, vol. 2020, Article ID 5086049, https://doi.org/10.1155/2020/5086049
6. Gambolati, G.; Teatini, P. Numerical Analysis of Land Subsidence Due to Natural Compaction of the Upper Adriatic Sea Basin. In CENAS - Coastline Evolution of the Upper Adriatic Sea Due to Sea Level Rise and Natural and Anthropogenic Land Subsidence; Gambolati, G., Ed.; Water Science and Technology Library: Dordrecht, 1998; Vol. 28, pp. 103–131, ISBN 978-94-011-5147-4. https://doi.org/10.1007/978-94-011-5147-4_5
7. Agavni Kaitantzian, Constantinos Loupasakis, Ploutarchos Tzampoglou, Isaak Parcharidis, "Ground Subsidence Triggered by the Overexploitation of Aquifers Affecting Urban Sites: The Case of Athens Coastal Zone along Faliro Bay (Greece)". *Geofluids*. **2020**. vol. 2020, Article ID 8896907, 1-18, https://doi.org/10.1155/2020/8896907
8. Loupasakis, C.; Rozos, D. Finite-Element Simulation of Land Subsidence Induced by Water Pumping in Kalochori Village, Greece. *Quarterly Journal of Engineering Geology and Hydrogeology* **2009**, 42, 369–382, https://doi.org/10.1144/1470-9236/08-022
9. Galloway, D.L.; Burbey, T.J. Review: Regional Land Subsidence Accompanying Groundwater Extraction. *Hydrogeology Journal* **2011**, 19, 1459–1486, https://doi.org/10.1007/s10040-011-0775-5
10. Pacheco-Martínez, J.; Hernandez-Marín, M.; Burbey, T.J.; González-Cervantes, N.; Ortíz-Lozano, J.Á.; Zermeño-De-Leon, M.E.; Solís-Pinto, A. Land Subsidence and Ground Failure Associated to Groundwater Exploitation in the Aguascalientes Valley, México. *Engineering Geology* **2013**, 164, 172–186, https://doi.org/doi:10.1016/j.enggeo.2013.06.015
11. Ezquerro, P.; Guardiola-Albert, C.; Herrera, G.; Fernández-Merodo, J.A.; Béjar-Pizarro, M.; Bonì, R. Groundwater and Subsidence Modeling Combining Geological and Multi-Satellite SAR Data over the Alto Guadalentín Aquifer (SE Spain). *Geofluids* **2017**, 2017, 1–17, https://doi.org/10.1155/2017/1359325
12. Tzampoglou, P.; Loupasakis, C. Numerical Simulation of the Factors Causing Land Subsidence Due to Overexploitation of the Aquifer in the Amyntaio Open Coal Mine, Greece. *HydroResearch* **2019**, 1, 8–24, https://doi.org/10.1016/j.hydres.2019.04.002
13. Sykioti, O., Kontoes, C. C., Elias, P., Briole, P., Sachpazi, M., Paradissis, D., Kotsis, I. Ground deformation at Nisyros volcano (Greece) detected by ERS-2 SAR differential interferometry, *International Journal of Remote Sensing* **2003**, 24:1, 183-188, https://doi.org/10.1080/01431160305000

14. Svigkas, N., Papoutsis, I., Loupasakis, C., Tsangaratos, P., Kiratzi, A., Kontoes, C. Land subsidence rebound detected via multi-temporal InSAR and ground truth data in Kalochori and Sindos regions, Northern Greece, *Engineering Geology* **2016**, 209, 175-186, https://doi.org/10.1016/j.enggeo.2016.05.017
15. Kontoes, C.; Loupasakis, C.; Papoutsis, I.; Alatza, S.; Poyiadji, E.; Ganas, A.; Psychogyiou, C.; Kaskara, M.; Antoniadi, S.; Spanou, N. Landslide Susceptibility Mapping of Central and Western Greece, Combining NGI and WoE Methods, with Remote Sensing and Ground Truth Data. *Land* **2021**, 10, 402. https://doi.org/10.3390/land10040402
16. Alatza, S.; Papoutsis, I.; Paradissis, D.; Kontoes, C.; Papadopoulos, G.A.; Raptakis, C. InSAR Time-Series Analysis for Monitoring Ground Displacement Trends in the Western Hellenic Arc: The Kythira Island, Greece. *Geosciences* **2020**, 10, 293. https://doi.org/10.3390/geosciences10080293
17. Papoutsis, I.; Kontoes, C.; Paradissis, D. Multi-Stack Persistent Scatterer Interferometry Analysis in Wider Athens, Greece. *Remote Sensing*, **2017**, 9, 276. https://doi.org/10.3390/rs9030276
18. Kontoes, C. (Haris); Alatza, S.; Chousianitis, K.; Svigkas, N.; Loupasakis, C.; Atzori, S.; Apostolakis, A. Coseismic Surface Deformation, Fault Modeling, and Coulomb Stress Changes of the March 2021 Thessaly, Greece, Earthquake Sequence Based on InSAR and GPS Data. *Seismological Research Letters* **2022**, 93, 2584–2598, https://doi.org/10.1785/0220210112
19. Alatza, S.; Papoutsis, I.; Paradissis, D.; Kontoes, C.; Papadopoulos, G.A. Multi-Temporal InSAR Analysis for Monitoring Ground Deformation in Amorgos Island, Greece. *Sensors* **2020**, 20, 338. https://doi.org/10.3390/s20020338
20. Ilia, I.; Loupasakis, C.; Tsangaratos, P. Land Subsidence Phenomena Investigated by Spatiotemporal Analysis of Groundwater Resources, Remote Sensing Techniques, and Random Forest Method: The Case of Western Thessaly, Greece., *Environmental Monitoring and Assessment* **2018**, 190, 1–19, https://doi.org/10.1007/s10661-018-6992-9
21. Tsangaratos, P.; Loupasakis, C.; Ilia, I. Ground Subsidence Phenomena in Frakadona, West Thessaly, Greece. In Proceedings of Fifth International Conference on Remote Sensing and Geoinformation of the Environment (RSCy2017) (Vol. 10444), 149–157, Paphos, Cyprus, 6 September 2017, https://doi.org/10.1117/12.2279082
22. Rozos, D.; Sideri, D.; Loupasakis, C.; Apostolidis, E. LAND SUBSIDENCE DUE TO EXCESSIVE GROUND WATER WITHDRAWAL. A CASE STUDY FROM STAVROS - FARSALA SITE, WEST THESSALY GREECE. *Bulletin of the Geological Society of Greece* **2010**, 43, 1850-1857. https://doi.org/10.12681/bgsg.11376
23. Raspini, F.; Loupasakis, C.; Rozos, D.; Adam, N.; Moretti, S. Ground Subsidence Phenomena in the Delta Municipality Region (Northern Greece): Geotechnical Modeling and Validation with Persistent Scatterer Interferometry. *International Journal of Applied Earth Observation and Geoinformation* **2014**, 28, 78–89, https://doi.org/10.1016/j.jag.2013.11.010
24. Svigkas, N.; Papoutsis, I.; Constantinos, L.; Tsangaratos, P.; Kiratzi, A.; Kontoes, C.H. Land Subsidence Rebound Detected via Multi-Temporal InSAR and Ground Truth Data in Kalochori and Sindos Regions, Northern Greece. *Engineering Geology* **2016**, 209, 175–186, ISSN 0013-7952, https://doi.org/10.1016/j.enggeo.2016.05.017
25. Svigkas, N.; Papoutsis, I.; Loupasakis, C.; Tsangaratos, P.; Kiratzi, A.; Kontoes, C.H. InSAR Time-Series Monitoring of Ground Displacement Trends in an Industrial Area (Oreokastro—Thessaloniki, Greece): Detection of Natural Surface Rebound and New Tectonic Insights. *Environmental Earth Sciences* **2017**, 76, 195, https://doi.org/10.1007/s12665-017-6517-9
26. Loupasakis, C.; Rozos, D. LAND SUBSIDENCE INDUCED BY THE OVEREXPLOITATION OF THE AQUIFERS IN KALOCHORI VILLAGE – NEW APPROACH BY MEANS OF THE COMPUTATIONAL GEOTECHNICAL ENGINEERING. *Bulletin of the Geological Society of Greece* **2010**, 43, 1219-1229. https://doi.org/10.12681/bgsg.11298
27. Svigkas, N.; Loupasakis, C.; Papoutsis, I.; Kontoes, C.; Alatza, S.; Tzampoglou, P.; Tolomei, C.; Spachos, T. InSAR Campaign Reveals Ongoing Displacement Trends at High Impact Sites of Thessaloniki and Chalkidiki, Greece. *Remote Sensing* **2020**, 12, 2396. https://doi.org/10.3390/rs12152396
28. Raspini, F.; Loupasakis, C.; Rozos, D.; Moretti, S. Advanced Interpretation of Land Subsidence by Validating Multi-Interferometric SAR Data: The Case Study of the Anthemountas Basin (Northern Greece). *Natural Hazards Earth System Sciences* **2013**, 13, 2425–2440, https://doi.org/10.5194/nhess-13-2425-2013
29. Raspini, F.; Bianchini, S.; Moretti, S.; Loupasakis, C.; Rozos, D.; Duro, J.; Garcia, M. Advanced Interpretation of Interferometric SAR Data to Detect, Monitor and Model Ground Subsidence: Outcomes from the ESA-GMES Terrafirma Project. *Natural Hazards* **2016**, 83, 155–181, https://doi.org/10.1007/s11069-016-2341-x
30. Svigkas, N.; Loupasakis, C.; Tsangaratos, P.; Papoutsis, I.; Kiratzi, A.; Kontoes, C. (Haris). A Deformation Study of Anthemountas Graben (Northern Greece) Based on in Situ Data and New InSAR Results. *Arabian Journal of Geosciences* **2020**, 13, 1–13, https://doi.org/10.1007/s12517-020-05393-9
31. Svigkas, N.; Papoutsis, I.; Loupasakis, C.; Tsangaratos, P.; Kiratzi, A.; Kontoes, C. (Haris). Radar Space Measurements of the Deforming Trends at Northern Greece Resulting from Underground Water Activity BT - Advances in Remote Sensing and Geo Informatics Applications.; El-Askary, H.M., Lee, S., Heggy, E.,

Pradhan, B., Eds.; Springer International Publishing: Cham, 2019; pp. 309–313. https://doi.org/10.1007/978-3-030-01440-7_70
32. Raspini, F.; Loupasakis, C.; Rozos, D.; Moretti, S. Basin and Local Scale Detection of Ground Subsidence through Persistent Scatterer Interferometry: The Anthemountas Basin (Northern Greece) Case Study. *Bulletin of the Geological Society of Greece* **2013**, 47, 1510-1518. https://doi.org/10.12681/bgsg.10989
33. Papoutsis, I.; Kontoes, C.; Alatza, S.; Apostolakis, A.; Loupasakis, C. InSAR Greece with Parallelized Persistent Scatterer Interferometry: A National Ground Motion Service for Big Copernicus Sentinel-1 Data. *Remote Sensing* **2020**, 12, 3207. https://doi.org/10.3390/rs12193207
34. Lemesios I. Environmental hydrogeological survey of the horizons of the wider area of the municipality of Messolonghi in relation to its natural healing resources. Master thesis, University of Patras, Patras, 2008, URL: https://hdl.handle.net/10889/823
35. Hellenic Survey of Geology & Mineral Exploration (HSGME). Geotechnical investigation of the foundations for the construction of worker's households in the areas of Messolonghi-Aitolikon I, II-Agrinio, **1987**, 5244, Technical Report
36. Hellenic Survey of Geology & Mineral Exploration (HSGME). Geological report on the Messolonghi lagoon drainage projects, **1958**, 654, Technical Report
37. Central Laboratory of Public Works. Messolonghi V – O.E.K., **1997**, 8.5 -118. Technical Report. Ministry of the Environment, Urban Planning and Public Works, Greece
38. Central Laboratory of Public Works. Geotechnical Investigation in O.E.K. site for the construction of worker's households in Messolonghi (Messolonghi V), **1997**, 8.5 -133, Technical Report. Ministry of the Environment, Urban Planning and Public Works, Greece
39. Douveas, N.; Kavadia, D.; Papadopoulou, P. Geotechnical Foundation Conditions of Mesologion Swimming Pool Center. *Bulletin of the Geological Society of Greece* **2007**, 40, 1644-1651. https://doi.org/10.12681/bgsg.17068
40. European Environment Agency, "Global and European Sea Level Rise", Available online: https://www.eea.europa.eu/ims/global-and-european-sea-level-rise (accessed on 25 September 2022).
41. Flanders Marine Institute (VLIZ). Intergovernmental Oceanographic Commission (IOC) (2022): Sea level station monitoring facility. Available online: https://www.ioc-sealevelmonitoring.org (accessed on 25 September 2022) at VLIZ https://doi.org/10.14284/482
42. Climate Change Knowledge Portal Greece, "Sea Level Rise" Available online: https://climateknowledgeportal.worldbank.org/country/greece/impacts-sea-level-rise (accessed on 25 September 2022)
43. NASA "Sea Level Projection Tool – NASA Sea Level Change Portal" Available online: https://sealevel.nasa.gov/ipcc-ar6-sea-level-projection-tool (accessed on 27 September 2022)
44. Lagouvardos, K.; Kotroni, V.; Bezes, A.; Koletsis, I.; Kopania, T.; Lykoudis, S.; Mazarakis, N.; Papagiannaki, K.; Vougioukas, S. The Automatic Weather Stations NOANN Network of the National Observatory of Athens: Operation and Database. *Geoscience Data Journal* **2017**, 4, 4–16, https://doi.org/10.1002/gdj3.44
45. Hooper, A.; Segall, P.; Zebker, H. Persistent Scatterer Interferometric Synthetic Aperture Radar for Crustal Deformation Analysis, with Application to Volcán Alcedo, Galápagos. *Journal of Geophysical Research* **2007**, 112, B07407, https://doi.org/10.1029/2006JB004763
46. Hellenic Mirror Site and the Sentinel Greek Copernicus Data Hubs. Available online: https://sentinels.space.noa.gr (accessed on 5 December 2022)
47. Bekaert, D.P.S.; Walters, R.J.; Wright, T.J.; Hooper, A.J.; Parker, D.J. Statistical Comparison of InSAR Tropospheric Correction Techniques. *Remote Sensing of Environment* **2015**, 170, 40–47, https://doi.org/10.1016/J.RSE.2015.08.035
48. Crosetto, M.; Solari, L.; Mróz, M.; Balasis-Levinsen, J.; Casagli, N.; Frei, M.; Oyen, A.; Moldestad, D.A.; Bateson, L.; Guerrieri, L.; Comerci, V.; Andersen, H.S. The Evolution of Wide-Area DInSAR: From Regional and National Services to the European Ground Motion Service. *Remote Sensing* **2020**, 12, 2043. https://doi.org/10.3390/rs12122043
49. Costantini, M.; Minati, F.; Trillo, F.; Ferretti, A.; Novali, F.; Passera, E.; Dehls, J.; Larsen, Y.; Marinkovic, P.; Eineder, M.; Brcic, R.; Siegmund, R.; Kotzerke, P.; Probeck, M.; Kenyeres, A.; Proietti, S.; Solari, L.; Andersen, H.S. EUROPEAN GROUND MOTION SERVICE (EGMS). In Proceedings of International Symposium on Geoscience and Remote Sensing (IGARSS), Brussels, Belgium, (11-16 July 2021), 3293–3296, https://doi.org/10.1109/igarss47720.2021.9553562
50. Groundwater Monitoring Network – DIPYN of HSGME. Available online: https://gaia.igme.gr/portal/apps/webappviewer/index.html?id=ba3251562a9f48dab498b8de2637afd3 (accessed on 28 November 2022).
51. © European Union, Copernicus Land Monitoring Service 2006, European Environment Agency (EEA)
52. © European Union, Copernicus Land Monitoring Service 2018, European Environment Agency (EEA)